Syntheses and Structural Characterization of Dinuclear and Trinuclear Iron(II) Complexes of Tridentate Thiolic Ligands with an NNS Donor Set

Masahiro Mikuriya,* Takanori Kotera, Fumiya Adachi, Makoto Handa,†
Masayuki Koikawa,††,# and Hisashi Ōkawa††

Department of Chemistry, School of Science, Kwansei Gakuin University, Uegahara, Nishinomiya 662

†Department of Chemistry, Faculty of Science, Shimane University, Matsue 690

††Department of Chemistry, Faculty of Science, Kyushu University 33, Hakozaki, Higashi-ku, Fukuoka 812

(Received July 4, 1994)

Thiolate-bridged complexes of iron(II) with 2-[(2-aminoethyl)amino]ethanethiol (HL_a), 2-[(3-aminopropyl)amino]ethanethiol (HL_b), and 2-[[2-(2-pyridyl)ethyl]amino]ethanethiol (HL_c) — $[Fe\{Fe(L_a)_2\}_2](ClO_4)_2\cdot CH_3OH$ (**1**), $[Fe\{Fe(L_b)_2\}_2]Cl_2\cdot 2CH_3OH$ (**2**), and $[Fe_2(L_c)_2(NO_3)_2]$ (**3**), respectively — have been synthesized and characterized by elemental analyses, and infrared and electronic spectroscopies as well as magnetic susceptibilities (80—300 K). The crystal structures of all of these complexes have been measured by single-crystal X-ray diffraction. Each of complexes **1** and **2** has a thiolate-bridged trinuclear iron(II) structure showing a linear arrangement of the three iron atoms with a geometry that may be described as *Oh-Td-Oh*. Complex **3** is a thiolate-bridged dinuclear iron(II) molecule, in which each iron atom is coordinated in a distorted octahedron. The electronic spectroscopic and magnetic properties are discussed in relation to the crystal structures.

Owing to the abundance of iron–sulfur clusters as prosthetic groups in a wide range of metallo-proteins, thiolate-bridged iron complexes are of tremendous interest.[1—8] Such interest in the iron thiolates has resulted in syntheses and characterization of mononuclear,[9—12] dinuclear,[13—19] trinuclear,[20—24] and tetranuclear[1—5,25—27] iron thiolates. However, compared to the tetranuclear complexes, relatively few dinuclear or trinuclear species have been reported for iron thiolates.[1—8] One of the difficulties in the syntheses of thiolate-bridged dinuclear or trinuclear complexes is due to the tendency of thiolic ligands to form polymeric complexes. Hence alkane thiols with tridentate NNS donor atoms such as 2-[[2-(2-pyridyl)ethyl]amino]ethanethiol are useful ligands to avoid such polymerization. In fact, we have shown that thiolate-bridged dinuclear nickel(II) complexes are formed by this type of ligands, and have confirmed their structures by X-ray crystal analysis.[28—34] Using the same type of ligands, HL, Handa et al. synthesized some thiolate-bridged iron(II) complexes (where HL denotes 2-[(2-aminoethyl)amino]ethanethiol, 2-[(2-pyridylmethyl)amino]ethanethiol, and 2-[[2-(2-pyridyl)ethyl]amino]-ethanethiol.[35] They proposed a dinuclear structure, $[Fe_2(L)_2Cl_2]$, for each of the iron(II) complexes obtained from the reaction of equimolar amounts of iron(II) chloride and HL. However, since their study was limited to only the chloro complexes and one method of synthesis, they were unable to obtain the trinuclear species. Furthermore, in the absence of X-ray crystallographic data, there was no definitive evidence for the structures. Therefore, in this study, we have aimed at establishing the structures of these thiolate-bridged iron(II) complexes. We have shown crystallographically that the reactions of Fe(II) with HL are dependent on the anionic ligands present in solution. The X-ray crystallographic work has shown the existence of novel thiolate-bridged trinuclear species besides the dinuclear complexes in this system. Here, we report the syntheses, X-ray crystal structures, spectral, and magnetic properties of the thiolate-bridged iron(II) complexes, $[Fe\{Fe(L_a)_2\}_2](ClO_4)_2\cdot CH_3OH$ (**1**), $[Fe\{Fe(L_b)_2\}_2]Cl_2\cdot 2CH_3OH$ (**2**), and $[Fe_2(L_c)_2(NO_3)_2]$ (**3**), where the thiolic ligands are 2-[(2-aminoethyl)amino]ethanethiol (HL_a), 2-[(3-aminopropyl)amino]ethanethiol (HL_b), and 2-[[2-(2-pyridyl)-ethyl]amino]ethanethiol (HL_c) (Chart 1). It is noteworthy that complex **3** is in line with the dinuclear species proposed earlier by Handa et al., the only difference being that it contains a nitrato ligand instead of a chloro ligand.

#Present address: Department of Chemistry, Faculty of Science and Engineering, Saga University, Saga 840.

HL_a: $H_2NCH_2CH_2NHCH_2CH_2SH$

HL_b: $H_2NCH_2CH_2CH_2NHCH_2CH_2SH$

HL_c:  $CH_2CH_2NHCH_2CH_2SH$

Chart 1.

Experimental

Syntheses of Complexes. The thiolic ligands — HL_a, HL_b, and HL_c — were synthesized by applying a method described in the literature.[30] All operations were done under an atmosphere of argon using standard Schlenk techniques.

$[Fe\{Fe(L_a)_2\}_2](ClO_4)_2\cdot CH_3OH$ (1). To a solution of HL_a (12 mg, 0.10 mmol) and sodium perchlorate (13 mg, 0.10 mmol) in methanol (4 cm^3) was added a methanol solution (1 cm^3) of iron(II) chloride tetrahydrate (20 mg, 0.10 mmol). The mixture was allowed to stand overnight to give brown plates. They were collected by filtration (yield 8.8 mg, 40%). Found: C, 22.81; H, 5.40; N, 12.59%. Calcd for $C_{17}H_{48}Cl_2Fe_3N_8O_9S_4$: C, 23.33; H, 5.53; N, 12.80%. IR (KBr) ν/cm^{-1} ν(NH) 3330(m), 3228(m); ν(CH) 2918(m), 2860(m); $\nu(ClO_4)$ 1143(s), 1105(s), 1087(s), 1028(s). Diffuse reflectance spectrum: λ_{max}/nm 310, 500sh, 750sh, 1135. μ_{eff} (297 K)/B.M. 7.23.

$[Fe\{Fe(L_b)_2\}_2]Cl_2\cdot 2CH_3OH$ (2). To a solution of iron(II) chloride tetrahydrate (75 mg, 0.38 mmol) in methanol (3 cm^3) was added a solution of HL_b (51 mg, 0.38 mmol) in a mixture of methanol (1 cm^3) and dimethylformamide (2 cm^3). The resulting solution was left for a few days to give brown plates. They were collected by filtration (yield 33 mg, 42%). Found: C, 31.28; H, 7.29; N, 13.11%. Calcd for $C_{22}H_{60}Cl_2Fe_3N_8O_2S_4$: C, 31.63; H, 7.23; N, 13.41%. IR (KBr) ν/cm^{-1} ν(NH) 3215(m), 3160(m); ν(CH) 2930(m), 2860(m). Diffuse reflectance spectrum: λ_{max}/nm 300, 370sh, 720sh, 1040. μ_{eff} (290 K)/B.M. 7.15.

$[Fe_2(L_c)_2(NO_3)_2]$ (3). To a methanol solution (4 cm^3) of iron(II) chloride tetrahydrate (75 mg, 0.38 mmol) and HL_c (69 mg, 0.38 mmol) was added a solution of sodium nitrate (32 mg, 0.38 mmol) in methanol (2 cm^3). The solution was left overnight to form brown plates (yield 43 mg, 38%). Anal. Found: C, 36.41; H, 4.59; N, 13.00%. Calcd for $C_{19}H_{30}Fe_2N_6O_7S_2$: C, 36.21; H, 4.80; N, 13.33%. IR (KBr) ν/cm^{-1} ν(NH) 3218(m); ν(CH) 2916(m), 2864(m); $\nu(NO_3)$ 1442(s), 1368(s), 1290(s). Diffuse reflectance spectrum: λ_{max}/nm 260, 400, 1000. μ_{eff} (299 K)/B.M. 6.69.

Measurements. Elemental analyses (C, H, and N) were done out using a Perkin–Elmer 2400 Series II CHNS/O Analyzer. Infrared spectra were measured with a JASCO Infrared Spectrophotometer Model IR700 in the region 4000—400 cm^{-1} as KBr disks. Diffuse reflectance spectra were recorded on a Shimadzu UV-vis-NIR Recording Spectrophotometer Model UV-3100. Magnetic susceptibilities were measured by the Faraday method over the 80—300 K temperature range. The apparatus was calibrated using $[Ni(H_2NCH_2CH_2NH_2)_3]S_2O_3$.[36] The susceptibilities were corrected for diamagnetism of the constituent atoms using Pascal's constants.[37] The effective magnetic moments were calculated from the equation $\mu_{eff}=2.828\sqrt{\chi_M T}$, where χ_M is the magnetic susceptibility per mole.

X-Ray Crystal Structure Analysis. Diffraction data were collected on an Enraf–Nonius CAD4 diffractometer using graphitemonochromated Mo $K\alpha$ radiation at 25±1 °C. Crystal data and details concerning data collection are given in Table 1. The lattice constants were calculated by a least-squares refinement based on 25 reflections with $20\leq 2\theta\leq 30°$. The intensity data were corrected for Lorentz-polarization effects, but not for absorption. The structures were solved by direct methods. Refinements were done by the full-matrix least-squares methods. Hydrogen atoms of **1** and **2** were fixed at their calculated positions. For **3**, hydrogen atoms were not included in the calculation. The weighting scheme, $w=1/[\sigma^2(|F_o|)+(0.02|F_o|)^2+1.0]$, was employed. The final discrepancy factors, $R=\sum||F_o|-|F_c||/\sum|F_o|$ and $R_w=[\sum w(|F_o|-|F_c|)^2/\sum w|F_o|^2]^{1/2}$, are listed in Table 1. All of the calculations were done on a Micro-VAXII computer using an Enraf–Nonius SDP program package.[38] The atomic coordinates and thermal parameters of the non-hydrogen atoms are listed in Table 2. The anisotropic thermal parameters of the non-hydrogen atoms, the atomic coordinates and temperature factors of the hydrogen atoms, and the F_o-F_c tables were deposited as Document No. 68001 at the Office of the Editor of Bull. Chem. Soc. Jpn.

Results and Discussion

Description of the Structures. $[Fe\{Fe(L_a)_2\}_2](ClO_4)_2\cdot CH_3OH$ (1). The crystal structure of **1** consists of a trinuclear cation, $[Fe\{Fe(L_a)_2\}_2]^{2+}$, two perchlorate ions, and a methanol molecule. A perspective view of $[Fe\{Fe(L_a)_2\}_2]^{2+}$ is illustrated in Fig. 1. The three iron atoms are nearly linear (Fe1–Fe3–Fe2= 172.0(1)°). The central iron atom, Fe3, has a distorted tetrahedral geometry, while the terminal iron atoms, Fe1 and Fe2, have distorted octahedral coordination spheres. The Fe1–Fe3 and Fe2–Fe3 distances of 3.153(3) and 3.117(3) Å, respectively, are too long for any metal–metal bonding (Table 3). The central Fe–S bond lengths [2.320(4)—2.341(5) Å] and S–Fe–S angles [104.3(2)—115.3(2)°] fall within the observed ranges for Fe–S bond distances [2.324(5)—2.396(3) Å] and S–Fe–S bond angles [95.6(1)—124.9(1)°], respectively, of tetrahedral Fe(II)–thiolate.[9—11] The thiolic

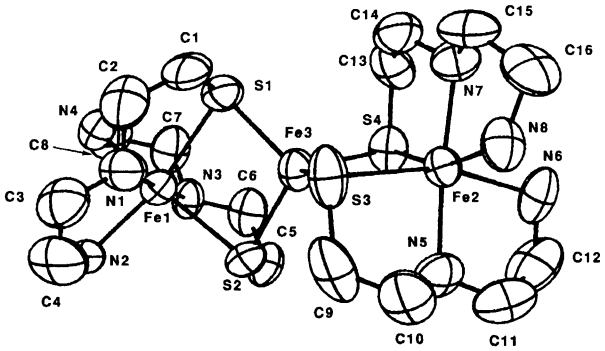

Fig. 1. Perspective view of trinuclear cation of $[Fe\{Fe(L_a)_2\}_2](ClO_4)_2\cdot CH_3OH$ (**1**).

Table 1. Crystal Data and Data Collection Details

Complexes	$[Fe\{Fe(L_a)_2\}_2](ClO_4)_2\cdot CH_3OH$ (**1**)	$[Fe\{Fe(L_b)_2\}_2]Cl_2\cdot 2CH_3OH$ (**2**)	$[Fe_2(L_c)_2(NO_3)_2]$ (**3**)
Formula	$C_{17}H_{48}Cl_2Fe_3N_8O_9S_4$	$C_{22}H_{60}Cl_2Fe_3N_8O_2S_4$	$C_{18}H_{26}Fe_2N_6O_6S_2$
F.W.	875.3	835.5	598.3
Crystal system	Monoclinic	Monoclinic	Monoclinic
Space group	$P2_1/c$	$C2/c$	$P2_1/c$
a/Å	16.837(3)	23.341(5)	8.504(4)
b/Å	15.318(3)	9.211(3)	16.945(4)
c/Å	14.294(6)	18.197(8)	8.685(4)
β/°	97.82(2)	103.50(2)	105.97(2)
V/Å^3	3652(2)	3804(2)	1203.3(8)
Z	4	4	2
D_c/g cm^{-3}	1.59	1.45	1.65
D_m/g cm^{-3}	1.57	1.37	1.60
$F(000)$	1816	1760	616
μ(Mo $K\alpha$)/cm^{-1}	15.9	15.1	14.2
Crystal dimensions/mm	$0.09\times0.30\times0.39$	$0.20\times0.22\times0.42$	$0.15\times0.20\times0.45$
2θ range/°	2.0—42.0	2.0—60.0	2.0—50.0
Total no. of observed reflections	4099	5864	2353
No. of unique reflections with $I>3\sigma(I)$	1987	2106	1269
Final no. of variables	388	186	154
Final rediduals			
R	0.058	0.069	0.060
R_w	0.061	0.073	0.069

ligand, L_a, forms a meridional bis-chelate with one thiolate sulfur atom and two amino nitrogen atoms coordinated to the terminal iron atom forming two adjacent five-membered chelate rings. The terminal Fe–S distances [2.497(5)—2.552(5) Å] are significantly longer than those of the central Fe–S. To date, there has been no report on structure analysis of octahedral Fe(II)–thiolates. The Fe–N bond lengths [2.18(1)—2.25(1) Å] compare well with those observed for the thiolate-bridged dinuclear iron(II) complexes of the tetradentate ligands with an N_2S_2 donor atom set [2.20(1)—2.337(7) Å].[16] To our knowledge, this is the first example of a structurally characterized linear trinuclear iron(II) complex displaying the geometry *Oh-Td-Oh*. The perchlorate ions are in the vicinity of the amino nitrogen atoms of the thiolic ligand as indicated by the distances O3(ClO_4)···N6 3.28(3) Å, O4(ClO_4)···N4 3.27(2) Å, O5(ClO_4)···N5 3.16(2) Å, and O9(ClO_4)···N4 3.17(2) Å which suggest the occurrence of hydrogen bonding. The methanol molecules are located near the perchlorate ions [O6(ClO_4)···O9(CH_3OH) 2.81(3) Å].

$[Fe\{Fe(L_b)_2\}_2]Cl_2\cdot 2CH_3OH$ (2). The crystal structure of **2** consists of a trinuclear cation, $[Fe\{Fe(L_b)_2\}_2]^{2+}$, two chloride ions, and two methanol molecules. A perspective view of $[Fe\{Fe(L_b)_2\}_2]^{2+}$ is illustrated in Fig. 2. The molecular structure of the complex cation is similar to that of **1**. The three iron atoms are linear (Fe2–Fe1–Fe2′=180°). The cation has C_2-symmetry with the crystallographic two-fold axis passing through Fe1 and the midpoint of S1 and S1′. The primed and unprimed atoms are related by C_2-

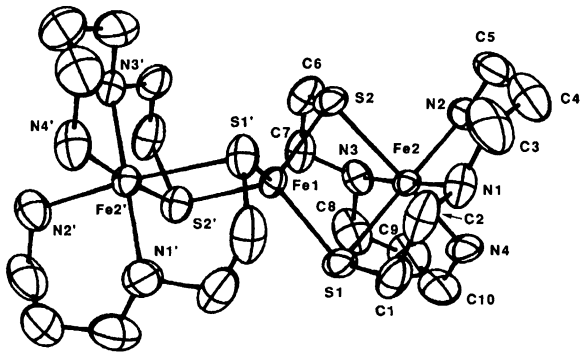

Fig. 2. Perspective view of trinuclear cation of $[Fe\{Fe(L_b)_2\}_2]Cl_2\cdot 2CH_3OH$ (**2**).

symmetry. The central iron atom, Fe1, has a distorted tetrahedral geometry, while the terminal iron atoms, Fe2 and Fe2′, have distorted octahedral geometries. The Fe1–Fe2 distance [3.311(1) Å] is significantly longer than those of **1** [3.153(3) and 3.117(3) Å]. The central Fe–S bond lengths [2.349(3), 2.362(3) Å] and S–Fe–S angles [100.88(9)—120.8(1)°] are comparable to those of tetrahedral Fe(II)–thiolates.[9—11] Each thiolic ligand, L_b, forms a fused 6—5 membered chelate ring in a meridional fashion. The terminal Fe–S distances are 2.546(3) and 2.584(3) Å. The Fe–N bond lengths are 2.18(1)—2.223(9) Å. These values are similar to those of **1**. However, the Fe–S–Fe angles [85.0(1), 83.9(1)°] are significantly larger than those of **1** [79.2(2)—81.7(1)°], resulting in the longer Fe–Fe distances. This may be due to the different size of the fused chelate ring. The chlo-

Table 2. Fractional Positional Parameters and Thermal Parameters of Nonhydrogen Atoms with Their Estimated Standard Deviations in Parentheses

Atom	x	y	z	B_{eq}/Å^2 a)
$[Fe\{Fe(L_a)_2\}_2](ClO_4)_2\cdot CH_3OH$ (**1**)				
Fe1	0.3102(1)	0.0817(1)	0.5124(1)	4.78(5)
Fe2	0.1520(1)	−0.2882(1)	0.4679(1)	4.57(5)
Fe3	0.2203(1)	−0.0994(2)	0.4961(2)	5.45(5)
Cl1	0.1042(3)	0.3751(3)	0.4015(4)	8.3(1)
Cl2	0.4692(3)	0.6418(4)	0.7183(3)	8.4(1)
S1	0.1640(3)	0.0385(3)	0.4637(3)	6.3(1)
S2	0.3529(2)	−0.0709(3)	0.5553(3)	5.4(1)
S3	0.2179(3)	−0.1853(3)	0.3610(3)	7.2(1)
S4	0.1475(3)	−0.1759(3)	0.5979(3)	6.0(1)
O1	0.1633(9)	0.418(1)	0.374(1)	20.9(6)
O2	0.098(1)	0.397(1)	0.489(1)	23.9(7)
O3	0.035(1)	0.397(1)	0.350(2)	24(1)
O4	0.109(1)	0.2898(9)	0.390(1)	15.4(7)
O5	0.4189(8)	0.693(1)	0.663(1)	12.6(4)
O6	0.521(1)	0.601(1)	0.670(1)	19.3(6)
O7	0.513(1)	0.689(1)	0.787(1)	19.3(8)
O8	0.432(1)	0.583(1)	0.765(1)	21.1(7)
O9	0.417(1)	0.339(1)	0.492(1)	16.0(6)
N1	0.3038(8)	0.074(1)	0.3542(9)	7.9(4)
N2	0.4319(7)	0.1292(8)	0.499(1)	6.7(4)
N3	0.3125(7)	0.0935(8)	0.6658(8)	5.5(3)
N4	0.2698(8)	0.2201(8)	0.5249(9)	6.6(4)
N5	0.2763(8)	−0.3379(8)	0.499(1)	7.1(4)
N6	0.1371(9)	−0.3989(8)	0.5658(9)	7.5(4)
N7	0.0265(7)	−0.2501(9)	0.4355(9)	6.3(4)
N8	0.1121(8)	−0.3723(8)	0.3425(8)	6.1(3)
C1	0.161(1)	0.048(1)	0.338(1)	9.1(6)
C2	0.226(1)	0.096(1)	0.311(1)	8.6(5)
C3	0.370(1)	0.123(1)	0.335(1)	8.9(6)
C4	0.442(1)	0.118(2)	0.394(1)	11.4(7)
C5	0.354(1)	−0.060(1)	0.683(1)	6.6(5)
C6	0.297(1)	0.010(1)	0.707(1)	7.2(5)
C7	0.256(1)	0.164(1)	0.681(1)	7.9(5)
C8	0.272(1)	0.243(1)	0.626(1)	8.4(6)
C9	0.316(1)	−0.241(1)	0.376(1)	10.0(5)
C10	0.313(1)	−0.332(1)	0.409(1)	8.7(5)
C11	0.274(1)	−0.423(1)	0.531(1)	8.1(5)
C12	0.219(1)	−0.427(1)	0.608(1)	10.1(6)
C13	0.0448(9)	−0.140(1)	0.560(1)	7.4(5)
C14	0.016(1)	−0.158(1)	0.454(1)	8.1(5)
C15	−0.001(1)	−0.274(1)	0.338(1)	8.1(5)
C16	0.024(1)	−0.368(1)	0.323(1)	8.2(5)
C17	0.446(2)	0.391(2)	0.564(2)	16.1(9)

Atom	x	y	z	B_{eq}/Å^2 a)
$[Fe\{Fe(L_b)_2\}_2]Cl_2\cdot 2CH_3OH$ (**2**)				
Fe1	0.000	0.0047(2)	0.250	2.85(3)
Fe2	0.12449(5)	0.0042(2)	0.38214(6)	2.76(2)
Cl	−0.8002(1)	0.5154(4)	0.4407(2)	5.84(7)
S1	0.0253(1)	0.1305(3)	0.3654(1)	4.23(6)
S2	0.0881(1)	−0.1238(3)	0.2533(1)	3.92(6)
O	−0.887(1)	0.402(2)	0.5374(9)	22.5(8)
N1	0.1508(4)	0.205(1)	0.3360(5)	5.0(2)
N2	0.2131(4)	−0.091(1)	0.3892(5)	5.1(2)
N3	0.0983(4)	−0.204(1)	0.4260(5)	4.2(2)
N4	0.1543(4)	0.086(1)	0.4992(5)	5.1(2)
C1	0.0547(5)	0.306(1)	0.3448(8)	5.9(3)
C2	0.0973(6)	0.292(1)	0.2959(7)	5.9(3)
C3	0.1937(6)	0.195(2)	0.2878(8)	8.7(4)
C4	0.2497(6)	0.116(2)	0.3266(8)	7.5(4)
C5	0.2459(5)	−0.043(2)	0.3315(7)	6.9(4)
C6	0.0815(5)	−0.298(1)	0.2970(7)	5.3(3)
C7	0.0564(5)	−0.286(1)	0.3657(7)	5.0(3)
C8	0.0730(6)	−0.188(2)	0.4954(7)	7.7(4)
C9	0.1179(6)	−0.118(2)	0.5611(6)	8.1(4)
C10	0.1226(6)	0.042(2)	0.5574(6)	7.4(4)
C11	−0.912(1)	0.443(3)	0.591(1)	17(1)
$[Fe_2(L_c)_2(NO_3)_2]$ (**3**)				
Fe	0.5811(2)	0.03960(7)	0.3597(2)	3.29(2)
S	0.3384(3)	−0.0448(2)	0.3446(3)	4.03(5)
O1	0.4387(8)	0.1523(4)	0.2898(9)	5.3(2)
O2	0.4754(9)	0.0808(5)	0.1040(9)	6.1(2)
N1	0.6621(9)	−0.0664(4)	0.270(1)	4.5(2)
N2	0.7965(8)	0.1038(4)	0.3283(9)	3.3(2)
N3	0.4135(8)	0.1393(3)	0.1550(8)	2.2(1)
O3	0.327(1)	0.1821(6)	0.048(1)	8.6(3)
C1	0.818(1)	0.1772(6)	0.391(1)	4.2(2)
C2	0.945(1)	0.2255(6)	0.381(1)	4.8(3)
C3	1.052(1)	0.1963(7)	0.301(1)	4.7(3)
C4	1.030(1)	0.1211(6)	0.236(1)	4.6(2)
C5	0.900(1)	0.0759(6)	0.251(1)	3.2(2)
C6	0.879(1)	−0.0055(6)	0.178(1)	4.1(2)
C7	0.838(1)	−0.0690(6)	0.285(1)	4.2(2)
C8	0.605(1)	−0.1349(6)	0.328(2)	6.4(3)
C9	0.423(1)	−0.1365(6)	0.289(1)	5.3(3)

a) Anisotropically refined atoms are given in the form of the isotropic equivalent thermal parameters defined as (4/3) $[a^2B_{11}+b^2B_{22}+c^2B_{33}+ac(\cos\beta)B_{13}]$.

ride ions and the methanol molecules are in the vicinity of the amino nitrogen atoms of the ligand as indicated by the distances Cl···N2 3.355(9) Å, Cl···O(CH_3OH) 3.15(2) Å, and O(CH_3OH)···N4 3.19(2) Å which point to the occurrence of hydrogen bonding.

$[Fe_2(L_c)_2(NO_3)_2]$ (3). The X-ray crystal structure shows that complex **3** is a thiolate-bridged dinuclear species (see Fig. 3). The primed and unprimed atoms are related by a center of symmetry. The Fe$\langle^{S}_{S'}\rangle$Fe′ core is a strict plane by the crystallographic symmetry. The thiolate-bridging mode is an "*anti*" configuration.[7] This is in marked contrast with the "*syn-endo*" configuration[7] of the thiolate-bridged dinuclear nickel(II) complexes where the Ni$\langle^{S}_{S}\rangle$Ni core has a bent structure resulting in the short Ni–Ni distances [2.69(1)—2.848(2) Å].[28,30,34] The Fe–Fe′ distance of 3.367(2) Å is comparable to the values of 3.206(5) and 3.371(2) Å found for other thiolate-bridged dinuclear iron(II) complexes, $[Fe_2(L_x)_2]$ and $[Fe_2(L_y)_2]$, where H_2L_x is *N*,*N*′-dimethyl-*N*,*N*′-bis(2-mercaptoethyl)eth-

Table 3. Selected Interatomic Distances (l/Å) and Bond Angles (ϕ/°) with Their Estimated Standard Deviations in Parentheses

$[Fe\{Fe(L_a)_2\}_2](ClO_4)_2 \cdot CH_3OH$ (**1**)			
Fe1–Fe2	6.255(3)	Fe1–Fe3	3.153(3)
Fe2–Fe3	3.117(3)	Fe1–S1	2.552(5)
Fe1–S2	2.497(5)	Fe1–N1	2.25(1)
Fe1–N2	2.21(1)	Fe1–N3	2.19(1)
Fe1–N4	2.24(1)	Fe2–S3	2.552(5)
Fe2–S4	2.541(5)	Fe2–N5	2.21(1)
Fe2–N6	2.23(1)	Fe2–N7	2.18(1)
Fe2–N8	2.24(1)	Fe3–S1	2.335(5)
Fe3–S2	2.320(4)	Fe3–S3	2.332(5)
Fe3–S4	2.341(5)		
Fe1–Fe3–Fe2	172.0(1)	S1–Fe1–S2	93.4(2)
S1–Fe1–N1	78.5(3)	S1–Fe1–N2	158.9(4)
S1–Fe1–N3	100.3(3)	S1–Fe1–N4	88.6(4)
S2–Fe1–N1	99.8(4)	S2–Fe1–N2	95.2(3)
S2–Fe1–N3	82.3(3)	S2–Fe1–N4	161.1(4)
N1–Fe1–N2	81.1(5)	N1–Fe1–N3	177.6(5)
N1–Fe1–N4	99.0(5)	N2–Fe1–N3	99.9(5)
N2–Fe1–N4	89.4(5)	N3–Fe1–N4	78.8(5)
S3–Fe2–S4	94.5(2)	S3–Fe2–N5	81.6(4)
S3–Fe2–N6	159.9(4)	S3–Fe2–N7	101.3(4)
S3–Fe2–N8	89.0(3)	S4–Fe2–N5	102.1(4)
S4–Fe2–N6	92.2(4)	S4–Fe2–N7	81.3(3)
S4–Fe2–N8	160.2(4)	N5–Fe2–N6	78.4(5)
N5–Fe2–N7	175.3(5)	N5–Fe2–N8	97.6(5)
N6–Fe2–N7	98.5(5)	N6–Fe2–N8	91.0(5)
N7–Fe2–N8	78.9(5)	S1–Fe3–S2	104.3(2)
S1–Fe3–S3	112.7(2)	S1–Fe3–S4	110.1(2)
S2–Fe3–S3	108.3(2)	S2–Fe3–S4	115.3(2)
S3–Fe3–S4	106.3(2)	Fe1–S1–Fe3	80.2(1)
Fe1–S2–Fe3	81.7(1)	Fe2–S3–Fe3	79.2(2)
Fe2–S4–Fe3	79.3(1)		

a) Primes refer to the equivalent positions ($-x$, y, $1/2-z$).

$[Fe\{Fe(L_b)_2\}_2]Cl_2 \cdot 2CH_3OH$ (**2**)[a]			
Fe1–Fe2	3.311(1)	Fe2–Fe2′	6.623(1)
Fe1–S1	2.349(3)	Fe1–S2	2.362(3)
Fe2–S1	2.546(3)	Fe2–S2	2.584(3)
Fe2–N1	2.18(1)	Fe2–N2	2.223(9)
Fe2–N3	2.222(9)	Fe2–N4	2.212(8)
S1–Fe1–S1′	120.8(1)	S1–Fe1–S2	100.88(9)
S1–Fe1–S2′	107.9(1)	S2–Fe1–S2′	119.8(1)
S1–Fe2–S2	90.15(9)	S1–Fe2–N1	84.0(3)
S1–Fe2–N2	174.6(3)	S1–Fe2–N3	96.9(2)
S1–Fe2–N4	91.9(3)	S2–Fe2–N1	95.9(2)
S2–Fe2–N2	88.7(2)	S2–Fe2–N3	82.5(2)
S2–Fe2–N4	172.5(3)	N1–Fe2–N2	90.9(4)
N1–Fe2–N3	178.2(4)	N1–Fe2–N4	91.5(4)
N2–Fe2–N3	88.2(4)	N2–Fe2–N4	89.9(3)
N3–Fe2–N4	90.1(3)	Fe1–S1–Fe2	85.0(1)
Fel–S2–Fe2	83.9(1)		

$[Fe_2(L_c)_2(NO_3)_2]$ (**3**)[b]			
Fe–Fe′	3.367(2)	Fe–S	2.522(3)
Fe–S′	2.419(3)	Fe–O1	2.264(7)
Fe–O2	2.227(8)	Fe–N1	2.146(8)
Fe–N2	2.242(8)		
S–Fe–S′	94.1(1)	S–Fe–O1	94.4(2)
S–Fe–O2	90.8(2)	S–Fe–N1	81.9(2)
S–Fe–N2	169.2(2)	S′–Fe–O1	102.9(2)
S′–Fe–O2	158.0(2)	S′–Fe–N1	111.8(2)
S′–Fe–N2	95.4(2)	O1–Fe–O2	55.3(3)
O1–Fe–N1	145.3(3)	O1–Fe–N2	88.5(3)
O2–Fe–N1	90.1(3)	O2–Fe–N2	82.3(3)
N1–Fe–N2	89.9(3)	Fe–S–Fe′	85.87(8)

b) Primes refer to the equivalent positions ($1-x$, $-y$, $1-z$).

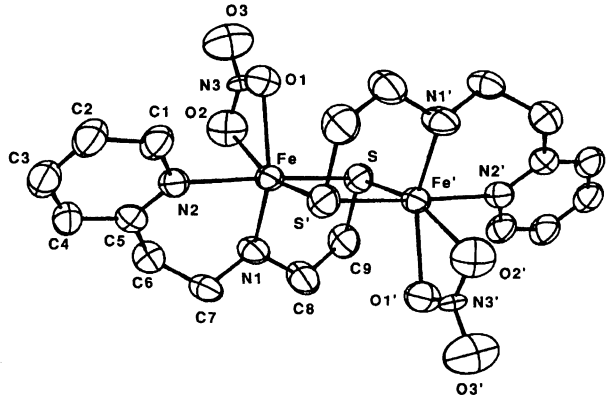

Fig. 3. Perspective view of $[Fe_2(L_c)_2(NO_3)_2]$ (**3**).

ylenediamine and H_2L_y is *N*,*N*′-dimethyl-*N*,*N*′-bis(2-mercaptoethyl)-1,3-propanediamine.[16] The coordination geometry about the iron atom is a distorted octahedron. Each thiolic ligand, L_c, acts as a meridional tridentate chelate forming a fused 5—6 chelate ring. The nitrate ion binds to the iron atom in a didentate fashion. This coordination mode is reflected in the infrared spectrum of **3** which shows a large splitting of the $\nu(NO_3)$ bands. The Fe–S and Fe–S′ distances are 2.522(3) and 2.419(3) Å, respectively. These values are comparable to those of the octahedral Fe(II)–thiolate found in **1** and **2**. The Fe–N1 [2.146(8) Å] and Fe–N2 [2.242(8) Å] distances compare well with the Fe–N bond lengths observed for the dinuclear iron(II) complexes, $[Fe_2(L_x)_2]$ and $[Fe_2(L_y)_2]$.[16] To our knowledge, this is the first example of a crystallographically analyzed dinuclear iron(II) complex with an *Oh*-*Oh* geometry.

Electronic Spectra and Magnetic Susceptibilities. The diffuse reflectance spectra of these complexes are shown in Fig. 4. The electronic spectra have an intense peak in the UV region, with a shoulder at 370—500 nm. This feature can be attributed to a thiolate-to-iron charge transfer transition.[9—11,20,22,23] In the visible region, a broad absorption band occurs at 1000—1135 nm. This band can be assigned to an iron(II) ligand field transition in *Oh*, $^5T_{2g} \rightarrow {}^5E_g$.[39] In the case of the trinuclear complexes **1** and **2**, an additional peak centered at longer wavelengths than 1500 nm is observed. This may be attributed to a ligand field transition in *Td*, $^5E \rightarrow {}^5T_2$.[39] These electronic spectral features are consistent with the structural data.

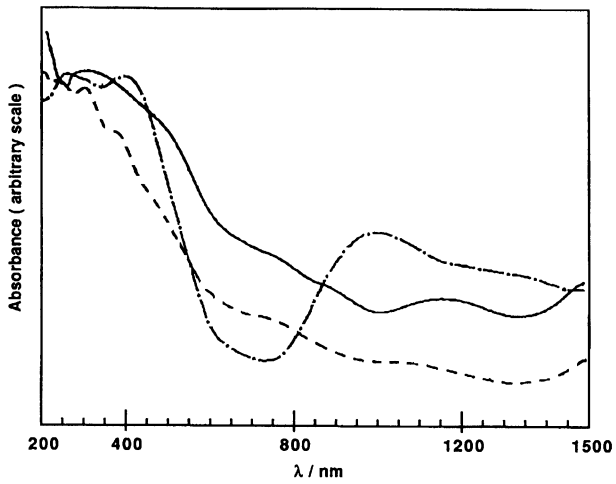

Fig. 4. Diffuse reflectance spectra of $[Fe\{Fe(L_a)_2\}_2]$-$(ClO_4)_2 \cdot CH_3OH$ (**1**) (—), $[Fe\{Fe(L_b)_2\}_2]Cl_2 \cdot 2CH_3$-OH (**2**) (---), and $[Fe_2(L_c)_2(NO_3)_2]$ (**3**) (-·-).

The effective magnetic moments of **1** and **2** are 7.23 and 7.15 B.M., respectively, at room temperature, showing values lower than the spin-only magnetic moment (8.49 B.M.) for a high-spin d^4–d^4–d^4 system. The magnetic susceptibilities were measured over the 80—300 K temperature range (Fig. 5). The magnetic data were analyzed by an isotropical Heisenberg model, $\mathscr{H} = -2J(S_1 \cdot S_2 + S_2 \cdot S_3) - 2J_{13} S_1 \cdot S_3$ assuming (1) the terminal and central iron(II) ions are all high-spin ($S_1 = S_2 = S_3 = 2$) and (2) the exchange interaction between nearest neighboring iron(II) ions are identical ($J = J_{12} = J_{23}$) and the interaction between the terminal iron(II) ions is negligible ($J_{13} = 0$). The resulting best fit parameters are $J = -46(2)$ cm^{-1}, $g = 2.24(1)$ for **1**;

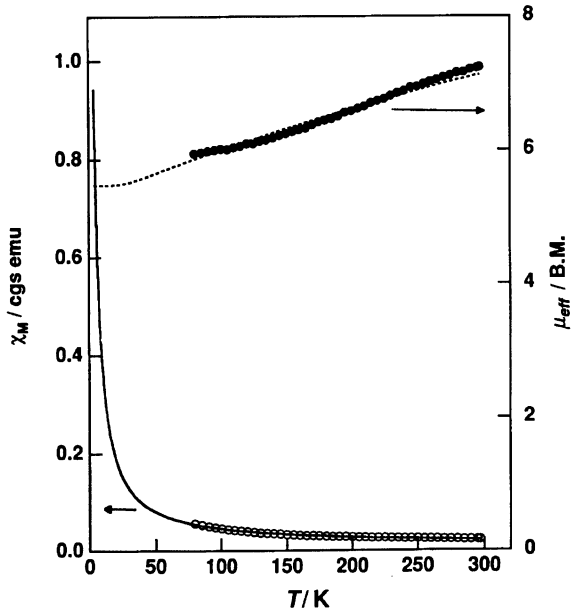

Fig. 5. Temperature dependence of the magnetic susceptibility (○) and effective magnetic moment (●) of $[Fe\{Fe(L_a)_2\}_2](ClO_4)_2 \cdot CH_3OH$ (**1**).

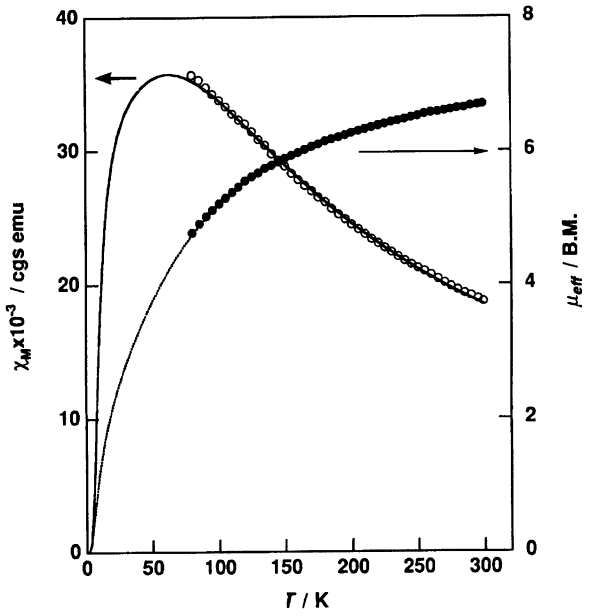

Fig. 6. Temperature dependence of the magnetic susceptibility (○) and effective magnetic moment (●) of $[Fe_2(L_c)_2(NO_3)_2]$ (**3**).

$J = -26(4)$ cm^{-1}, $g = 1.97(6)$ for **2**. The considerable antiferromagnetic exchange interaction occurs through the bridging thiolate groups. On the other hand, the magnetic moment of **3** (6.69 B.M. at 299 K) is also lower than the spin-only magnetic moment (6.92 B.M.) for high-spin d^4–d^4 system and the magnetic data could be explained by the dimer equation ($S_1 = S_2 = 2$) based on the Heisenberg model, $\mathscr{H} = -2J S_1 \cdot S_2$. The best fit with $g = 2.137(2)$ and $J = -10.02(4)$ cm^{-1} is shown as the solid line in Fig. 6. The antiferromagnetic interaction between the Fe and Fe′ atoms through the thiolate bridges is rather weak compared with those observed for the trinuclear complexes **1** and **2**. The fairly large antiferromagnetic coupling between the iron atoms in the trinuclear complexes may be due to the shorter Fe–Fe distances.

References

1) R. H. Holm and J. A. Ibers, "Iron-Sulfur Proteins," in "Metal Ions in Biology," ed by W. Lovenberg, Academic, New York (1977), Vol. 3.

2) J. M. Berg and R. H. Holm, "Iron-Sulfur Proteins," in "Metal Ions in Biology," ed by T. G. Spiro, Wiley-Interscience, New York (1982), Vol. 4.

3) R. H. Holm, *Acc. Chem. Res.*, **10**, 427 (1977).

4) R. H. Holm, *Chem. Soc. Rev.*, **10**, 455 (1981).

5) R. H. Holm, S. Ciurli, and J. A. Weigel, *Prog. Inorg. Chem.*, **38**, 1 (1990).

6) I. G. Dance, *Polyhedron*, **5**, 1037 (1986).

7) P. J. Blower and J. R. Dilworth, *Coord. Chem. Rev.*, **76**, 121 (1987).

8) V. B. Krebs and G. Henkel, *Angew. Chem.*, **103**, 785 (1991).

9) R. W. Lane, J. A. Ibers, R. B. Frankel, and R. H.

Holm, *Proc. Natl. Acad. Sci. U.S.A.*, **72**, 2868 (1975).
10) R. W. Lane, J. A. Ibers, R. B. Frankel, G. C. Papaefthymiou, and R. H. Holm, *J. Am. Chem. Soc.*, **99**, 84 (1977).
11) D. Coucouvanis, D. Swenson, N. C. Baenziger, C. Murphy, D. G. Holah, N. Sfarnas, A. Simounopoulos, and A. Kostikas, *J. Am. Chem. Soc.*, **103**, 3350 (1981).
12) S. A. Koch, L. E. Maelia, and M. Millar, *J. Am. Chem. Soc.*, **105**, 5944 (1983).
13) J. J. Mayerle, R. B. Frankel, R. H. Holm, J. A. Ibers, W. D. Phillips, and J. F. Weiher, *Proc. Natl. Acad. Sci. U.S.A.*, **70**, 2429 (1973).
14) J. J. Mayerle, S. E. Denmark, B. V. DePamphilis, J. A. Ibers, and R. H. Holm, *J. Am. Chem. Soc.*, **97**, 1032 (1975).
15) M. R. Snow and J. A. Ibers, *Inorg. Chem.*, **12**, 249 (1973).
16) W. -J. Hu and S. J. Lippard, *J. Am. Chem. Soc.*, **96**, 2366 (1974).
17) K. Hagen and R. H. Holm, *Inorg. Chem.*, **23**, 418 (1984).
18) G. Henkel, W. Tremel, and B. Krebs, *Angew. Chem.*, **95**, 317 (1983).
19) P. P. Power and S. C. Shoner, *Angew. Chem., Int. Ed. Engl.*, **30**, 330 (1991).
20) G. Henkel, W. Tremel, and B. Krebs, *Angew. Chem.*, **93**, 1072 (1981).
21) K. S. Hagen and R. H. Holm, *J. Am. Chem. Soc.*, **104**, 5496 (1982).
22) K. S. Hagen, G. Christou, and R. H. Holm, *Inorg. Chem.*, **22**, 309 (1983).
23) K. S. Hagen, A. D. Watson, and R. H. Holm, *J. Am. Chem. Soc.*, **105**, 3905 (1983).
24) M. A. Whitener, J. K. Bashkin, K. S. Hagen, J.-J. Girerd, E. Gamp, N. Edelstein, and R. H. Holm, *J. Am. Chem. Soc.*, **108**, 5607 (1986).
25) K. S. Hagen, J. M. Berg, and R. H. Holm, *Inorg. Chim. Acta*, **45**, L17 (1980).
26) D. Coucouvanis, M. Kanatzidis, E. Simhon, and N. C. Baenziger, *J. Am. Chem. Soc.*, **104**, 1874 (1982).
27) K. S. Hagen, D. W. Stephen, and R. H. Holm, *Inorg. Chem.*, **21**, 3928 (1982).
28) M. Mikuriya, S. Kida, and I. Murase, *Bull. Chem. Soc. Jpn.*, **60**, 1180 (1987).
29) M. Handa, M. Mikuriya, H. Okawa, and S. Kida, *Chem. Lett.*, **1988**, 1555.
30) M. Handa, M. Mikuriya, Z. J. Zhong, H. Okawa, and S. Kida, *Bull. Chem. Soc. Jpn.*, **61**, 3883 (1988).
31) M. Handa, M. Mikuriya, and H. Okawa, *Chem. Lett.*, **1989**, 1663.
32) M. Mikuriya, S. Shigematsu, M. Handa, and T. Kohzuma, *Transition Met. Chem. (Weinheim, Ger.)*, **16**, 532 (1991).
33) M. Mikuriya, M. Handa, S. Shigematsu, S. Funaki, F. Adachi, and H. Okawa, *Bull. Chem. Soc. Jpn.*, **65**, 512 (1992).
34) M. Mikuriya, M. Handa, S. Shigematsu, S. Funaki, T. Fujii, H. Okawa, K. Toriumi, T. Koshiba, and H. Terauchi, *Bull. Chem. Soc. Jpn.*, **66**, 1104 (1993).
35) M. Handa, H. Okawa, and S. Kida, *Bull. Chem. Soc. Jpn.*, **61**, 3353 (1988).
36) N. F. Curtis, *J. Chem. Soc.*, **1961**, 3147.
37) P. W. Selwood, "Magnetochemistry," Interscience Publishers, New York (1956), pp. 78 and 91.
38) B. A. Frenz, "The SDP-User's Guide," Enraf-Nonius, Delft, The Netherlands (1985).
39) A. B. P. Lever, "Inorganic Electronic Spectroscopy," Elsevier, Amsterdam (1984).